Biosynthesis Hot Paper

How to cite:
International Edition: doi.org/10.1002/anie.202107192
German Edition: doi.org/10.1002/ange.202107192

Post-Translational Formation of Aminomalonate by a Promiscuous Peptide-Modifying Radical SAM Enzyme

*Suze Ma[+], Heng Chen[+], He Li, Xinjian Ji, Zixin Deng, Wei Ding, and Qi Zhang**

Abstract: *Aminomalonate (Ama) is a widespread structural motif in Nature, whereas its biosynthetic route is only partially understood. In this study, we show that a radical S-adenosylmethionine (rSAM) enzyme involved in cyclophane biosynthesis exhibits remarkable catalytic promiscuity. This enzyme, named three-residue cyclophane forming enzyme (3-CyFE), mainly produces cyclophane in vivo, whereas it produces formylglycine (FGly) as a major product and barely produce cyclophane in vitro. Importantly, the enzyme can further oxidize FGly to produce Ama. Bioinformatic study revealed that 3-CyFEs have evolved from a common ancestor with anaerobic sulfatase maturases (anSMEs), and possess a similar set of catalytic residues with anSMEs. Remarkably, the enzyme does not need leader peptide for activity and is fully active on a truncated peptide containing only 5 amino acids of the core sequence. Our work discloses the first ribosomal path towards Ama formation, providing a possible hint for the rich occurrence of Ama in Nature.*

Introduction

Aminomalonate (Ama), the structural congener of aspartate and glutamate, is a long known metabolite in Nature and was proposed to be an intermediate in glycine biosynthesis.[1,2] Ama has been found in several natural products,[3–7] and can also serve as an extender unit in the biosynthesis of polyketides and/or non-ribosomal peptides (Figure S1).[8–11] Ama was also found as an important constituent in the *Escherichia coli* (*E. coli*) protein hydrolysate, and is likely widespread in various proteomes.[12,13] Post-translational modifications, such as α-carboxylation of glycine, and over-oxidation of Ser,[13] have been hypothesized to produce Ama in a ribosomally synthesized polypeptide, but thus far none of these feasibilities have been experimentally validated.

Ribosomally synthesized and post-translationally modified peptides (RiPPs) afford fascinating opportunities to discover novel biochemistries.[14,15] Particularly, the radical S-adenosylmethionine (rSAM) superfamily enzymes are extensively involved in RiPP biosynthesis and catalyze strikingly diverse reactions.[16,17] The rSAM-dependent RiPPs include sactipeptide (α-thioether linkage),[18–20] ranthipeptide (β or γ-thioether linkage),[21–23] streptide (C–C crosslink between Lys and Trp),[24] rotapeptide (C-O crosslink between Thr and Gln)[25] and ryptide (C–C crosslink between Arg and Tyr),[26] among others. In these reactions, the rSAM enzymes utilize a strictly conserved [4Fe-4S] cluster to reductively cleave S-adenosylmethionine (SAM), and the resulting 5′-deoxyadenosyl (dAdo) radical abstracts a hydrogen atom from the substrate to initiate subsequent oxidation reactions.[27,28] In addition, the RiPP-modifying rSAM enzymes contain a characteristic C-terminal extension called SPASM domain, which accommodates one or more additional [4Fe-4S] clusters, with roles suggestive of peptide binding or electron transfer.[29]

In silico analysis of novel rSAM-dependent RiPPs with the aid of co-expression in *E. coli* proves to be fruitful in exploring novel rSAM enzymes and their substrate specificity.[30] A recent study showed that a group of rSAM enzymes catalyze the crosslinking between an aromatic residue (Ω1) and a non-aromatic residue (X3) in a Ω1-X2-X3 motif to produce a cyclophane moiety.[31] These enzymes are hence defined as three-residue cyclophane-forming enzymes (3-CyFEs). 3-CyFEs are abundant in diverse bacterial phyla and can be further classified into different clades based on the characteristic motif of substrate, such as Xye (TIGR04495), Grr (TIGR04260) and Fxs (TIGR04268).[31] Xye is named for its wide distribution in strains of the genera *Xenorhabdus*, *Yersinia* and *Erwinia.* Grr system denotes that the precursor peptide contains multiple glycine-rich repeats. Fxs contains a highly conserved substrate tail F-X-S-X-X-COOH. These 3-CyFE-derived RiPPs were designated as triceptide (three-residue in cyclophane peptides).[31] In this study, we report detailed in vitro characterization of a 3-CyFE involved in the biosynthesis of a Fxs-type triceptide. We show that unexpectedly, the enzyme did not catalyze cyclophane formation in vitro. Instead, it catalyzes oxidation of the Ser in the Ω1-X2-S3 motif to produce formylglycine (FGly) and Ama. We further show that 3-CyFEs have evolved from a common ancestor with anaerobic sulfatase maturases (anSMEs), and both groups of enzymes possess a similar set of catalytic residues. In constrast to most RiPP biosynthetic enzymes, 3-CyFE does not require leader peptide for activity.

[*] S. Ma,[+] H. Chen,[+] H. Li, Dr. X. Ji, Prof. Dr. Q. Zhang
Department of Chemistry, Fudan University
Shanghai, 200433 (China)
E-mail: qizhang@sioc.ac.cn

Prof. Dr. Z. Deng, Prof. Dr. W. Ding
State Key Laboratory of Microbial Metabolism, School of Life Sciences & Biotechnology, Shanghai Jiao Tong University
Shanghai, 200240 (China)

[+] These authors contributed equally to this work.

Supporting information and the ORCID identification number(s) for the author(s) of this article can be found under: https://doi.org/10.1002/anie.202107192.

Results and Discussion

The sji Biosynthetic Cluster

RiPPs are derived from gene-encoded precursor peptides consisting of an N-terminal leader and a C-terminal core. In most cases, the leader peptide is recognized by a small structural domain called RiPP recognition element (RRE), which directs the interaction between substrate and the modifying enzymes.[32,33] RRE is indispensable for most RiPP-modifying rSAMs known thus far,[34–37] which can be found either as an N-terminal extension domain or as a standalone polypeptide encoded in the biosynthetic gene cluster (BGC) (Table S2).

In an in silico analysis (Table S2), we occasionally noted the RRE domain seems to be absent in tricepeptide biosynthesis, as it is neither found in 3-CyFEs, nor encoded in the corresponding BGCs. Intrigued by this observation, we focused on a putative Fxs gene cluster (hereafter termed *sji*, Figure 1A and Note S1) from *Streptacidiphilus jiangxiensis*, an actinomycete from acidic rhizosphere soil in China.[39] This gene cluster encodes a 60-aa precursor peptide SjiA, whose C-terminal sequence FQSSI is characteristic of the FxS substrate motif. The cluster also encodes a putative 3-CyFE SjiB.

We first set out to validate the enzyme activity by a co-expression approach, similar to the recent report by Morinaka et al.[31] To this end, SjiA was co-expressed with the rSAM/SPASM domain of SjiB (hereafter termed SjiB-399) in *E. coli*, and the product was purified by Ni^{2+} affinity chromatography. Liquid chromatography with high-resolution mass spectrometry (LC-HRMS) analysis showed the resulting SjiA is 2 Da less ($[M+8H]^{8+}=819.31$) compared to the unmodified SjiA obtained by expressing SjiA alone ($[M+8H]^{8+}=819.56$) (Figure 1B). The in vivo modified peptide was then digested by trypsin and analyzed by high-resolution tandem MS (HR-MS/MS), and the result clearly revealed that the tryptic fragment **$SjiA_{51–60}$** ($[M+H]^{+}=1034.51$) contains a crosslink between the conserved Phe and Ser as previously characterized (Figure 1C and Figure S2). We hereafter refer to the crosslinked SjiA as **1**, and the tryptic fragment was accordingly termed **$SjiA_{51–60}$-1**.

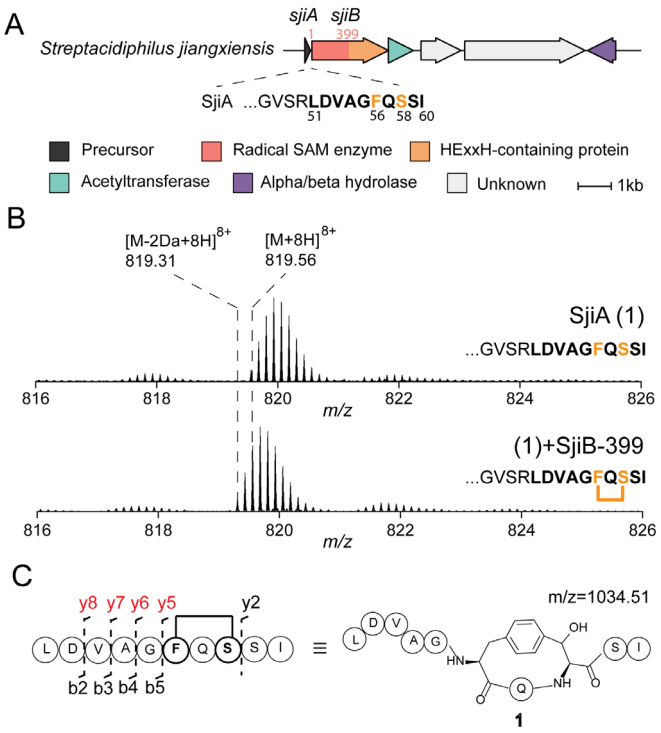

Figure 1. The *sji* gene cluster and its cyclophane product. (A) The *sji* biosynthetic gene cluster encodes a precursor peptide SjiA and a FxsB-type 3-CyFE SjiB. As the boundary between leader and core in SjiA is currently unknown, we only showed the C-terminus of SjiA, with the tryptic sequence highlighted in bold. See Note S1 for detailed sequences. SjiB consists of an N-terminal SPASM family of rSAM domain and a C-terminal HExxH domain; the latter domain was suggestive of metalloprotease activity.[31,38] (B) HR-MS characterization of SijA modified by SjiB-399 in vivo (**1**). The loss of 2 Da is a result of C–C crosslink in cyclophane formation. (C) HR-MS/MS characterization of the tryptic sequence **$SjiA_{51–60}$–61**. The *y* ions in red correspond to the −2 Da mass change resulting from the C–C crosslink.

In Vitro Activity of SjiB-399

After validating the activity of SjiB-399 in vivo, we prepared SjiA and SjiB-399 separately for in vitro characterization. SjiB-399 was purified to near homogeneity under strictly anaerobic condition, followed by chemical reconstitution and gel filtration (Figure S9). The ultraviolet-visible (UV/Vis) absorption spectrum of the chemically reconstituted SjiB-399 revealed a broad feature at 410 nm (Figure 2A), suggestive of the presence of one or more $[4Fe\text{-}4S]^{2+}$ clusters. Quantification analysis showed that each enzyme contains 7.5 ± 0.4 iron and 7.3 ± 0.5 labile sulfide, suggesting it harbors two [4Fe-4S] clusters. We next anaerobically incubated SjiB-399 with SAM and sodium dithionite (DTH) in the absence of SjiA. This assay revealed a time-dependent production of 5′-deoxyadenosine (dAdoH) (Figure 2B and Figure S10), indicating that SjiB-399 is indeed a rSAM protein.

To reconstitute the enzyme activity in vitro, we treated SjiA with SjiB-399, SAM and DTH under strictly anaerobic condition, and the reaction mixture was analyzed by LC-HRMS. In this analysis, we observed a major product with the expected −2 Da monoisotopic peak ($[M+8H]^{8+}=819.31$), and two minor products with isotopically mixed mass signals at +14 and +16 Da (i.e. $[M+8H]^{8+}=821.31$ and 821.56, Figure 2C). Trypsin digestion ascertained the three products, which exhibit −2, +14, +16 Da mass change, respectively (correspond to $[M+H]^{+}=1034.51$, 1050.51, and 1052.52, respectively) (Figure S12). Unexpectedly, extracted ion chromatography (EIC) showed that the −2 Da species produced in vitro (hereafter referred to as **2**) is apparently different from **1** obtained in vivo, as the focused tryptic fragment of **2** (hereafter **$SjiA_{51–60}$-2**) is eluted ≈20 sec latter in LC-MS analysis (Figure 2D). Careful re-examination showed that **2** was also produced in vivo, with a yield ≈10-fold lower than that of **1** (Figure 2D, Figure S11 and S17).

The apparent difference of **2** and **1** indicates **2** contains a distinct modification. Comparative HR-MS/MS analysis of the two tryptic fragments showed that, in contrast to **$SjiA_{51–60}$-**

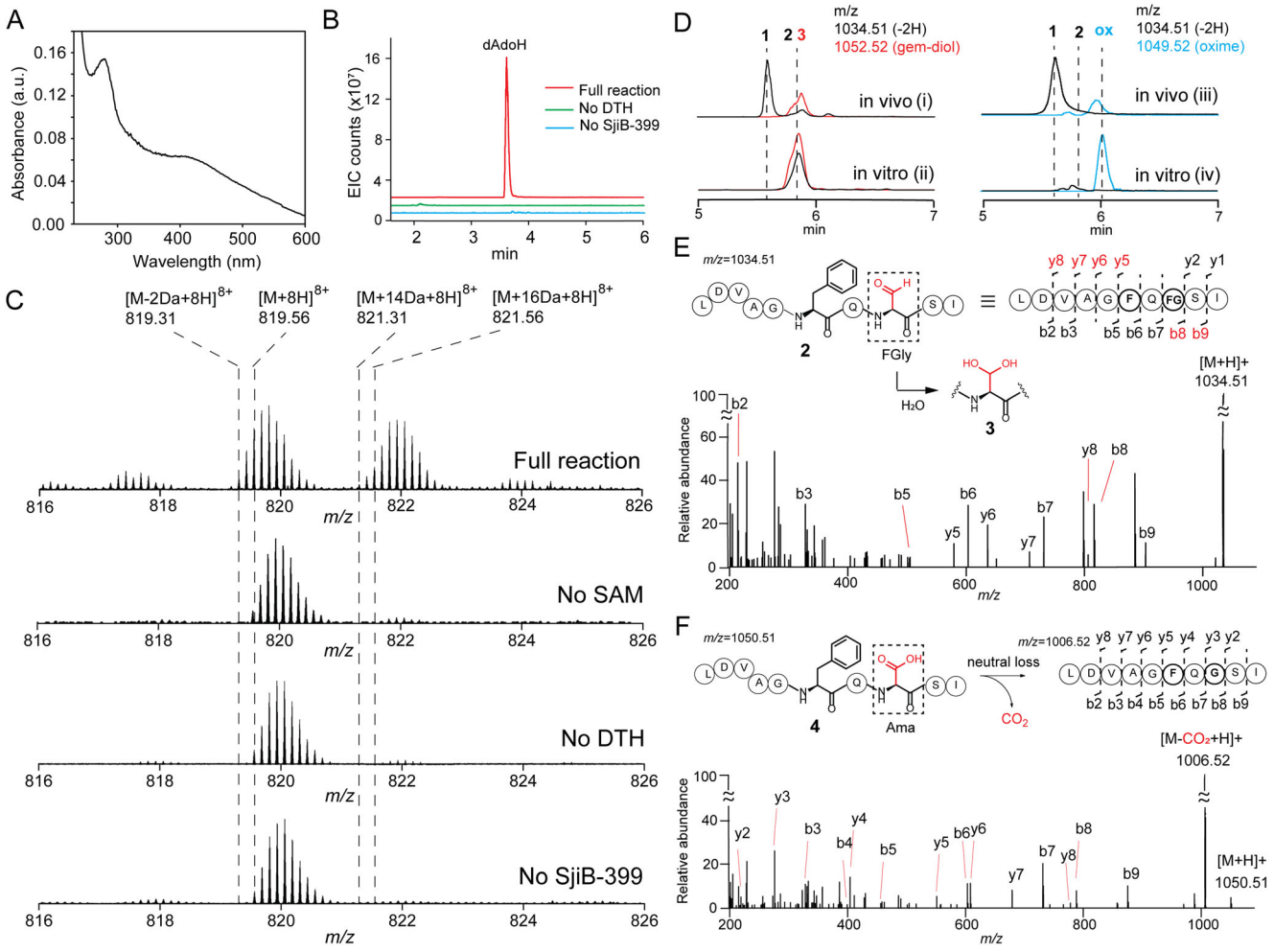

Figure 2. In vitro characterization of SjiB-399 reveals the production of FGly and Ama-containing peptide. A. UV/Vis spectrum of the chemically reconstituted SjiB-399. B. The extracted ion chromatograms (EICs) of SjiB-399-catalyzed dAdoH production. C. HR-MS analysis of SjiA peptide treated with purified SjiB-399 in vitro. The full reaction was carried out with 50 μM SjiA, 5 μM reconstituted SjiB-399, 2 mM SAM, and 10 mM DTH; the three control assays omit SAM, DTH, and SjiB-399, respectively. The full reaction catalyzed by SjiB-399 produce a major product with −2 Da, and two minor products with +14 Da and +16 Da. D. EICs for the tryptic products obtained from (i) in vivo co-expression and (ii) in vitro reaction, as well as NH_2OH-treatment of the (iii) in vivo and (iv) in vitro products. ox denotes the oxime derivative of **2** and **3**. E. HR-MS/MS dissection of the FGly-containing peptide **2**. Note that FGly can be hydrated to yield the gem-diol counterpart **3**. F. HR-MS/MS dissection of the Ama-containing peptides **4**, showing a CID-mediated decarboxylation-type of neutral loss and the corresponding fragmentation.

1, **SjiA$_{51–60}$-2** exhibited a series of b and *y* ions within the to-be-cyclized FxS motif (Figure 2E and Figure S3), indicating that the FxS motif was not cross-linked in **2**. More importantly, the −2 Da modification was observed exclusively on the Ser residue within the FxS motif (Figure 2E), which is reminiscent of formylglycine (FGly), a structural motif can be formed by anaerobic sulfatase maturation enzyme (anSME).[40–42] This proposal is consistent with the observation of the +16 Da (i.e. $[M + H]^+ = 1052.52$) product, a putative *gem*-diol (**3**) formed via hydration of **2.** Indeed, **SjiA$_{51-60}$-3** is eluted simultaneously with **SjiA$_{51–60}$-2** in the LC-MS analysis (Figure 2D), and displayed exactly the same MS/MS fragmentation pattern as that of **SjiA$_{51–60}$-2** (Figure S4). To further verify the structure of **2** and **3**, we treated the tryptic products from both in vivo and in vitro studies with sodium borohydride ($NaBH_4$) and hydroxylamine (NH_2OH). In this analysis, **SjiA$_{51–60}$-2** and **SjiA$_{51–60}$-3** were completely reduced or converted to the oxime-derivative, whereas the **SjiA$_{51–60}$-1** remain unchanged (Figure 2D, Figure S6-S8). These results confirmed FGly production in the SjiB-399-catalyzed reaction.

rSAM-Dependent Ama Formation in SjiA

For the +14 Da product (i.e. $[M + H]^+ = 1050.51$, **SjiA$_{51–60}$-4)**, HR-MS/MS analysis revealed a set of b and *y* ions that do not match the **SjiA$_{51–60}$** sequence. However, we noticed the monoisotopic peak at $m/z = 1006.52$ is the most intensive peak in the spectrum, which is 44 Da less compared to the parent ion (i.e. $m/z = 1050.52$), suggesting a decarboxylation-type neutral loss in MS/MS analysis (Figure 2F and Figure S5). This type of neutral loss has not been observed for peptidyl moiety produced by common post-translational

modifications,[43] but is reminiscent of Ama, a malonate-containing amino acid.[44,45] We hence speculated that **SjiA$_{51-60}$-4** contains a Ser-derived Ama, which was decarboxylated to produce a Gly during collision-induced dissociation (CID) in HR-MS/MS analysis. Consistent with this proposal, the HR-MS/MS spectrum of **SjiA$_{51-60}$-4** matches well to a Ser-to-Gly mutant of **SjiA$_{51-60}$** (i.e. the ion with $[M+H]^+ = 1006.52$), in which the Ser residue in the FxS motif is changed to a Gly.

To validate the CID-induced decarboxylation of Ama, we obtained Ama according to a previous report[13] and performed MS/MS analysis with the same instrumental setting. This analysis clearly shows that Ama underwent decarboxylation efficiently (Figure S13), which is consistent with the fragmentation pattern observed for **SjiA$_{51-60}$-4.** To unambiguously characterize the Ama in **SjiA$_{51-60}$-4**, we carried out the SjiB-399-catalyzed in vitro reaction in large scale, and the product was subjected to alkaline hydrolysis, followed by phenyl isothiocyanate (PITC) derivatization. LC-HRMS analysis showed the expected product was co-eluted with the authentic Ama derivative (Figure S14), confirming the production of Ama in the assay.

We hypothesized the Ama is likely produced by over-oxidation of the Ser residue by SjiB-399, which likely involves the *gem*-diol intermediate **3** (Figure 2E). To test this proposal, we ran the reaction in 70% $H_2{}^{18}O$, and the resulting product was treated with trypsin and analyzed by LC-HRMS. This analysis clearly indicated that up to two ^{18}O atoms can be incorporated into **SjiA$_{51-60}$-4**, showing two newly formed species at $[M + H]^+ = 1052.51$ and $[M + H]^+ = 1054.52$, respectively (Figure 3A). Selected ion monitoring (SIM) followed by HR-MS/MS analysis of the two species showed that the HR-MS/MS spectra display an invariant daughter ion (i.e. $[M + H]^+ = 1006.52$) (Figure S15) as well as corresponding b and *y* ions. The enriched ^{18}O signal is present in the parent ion but is absent in the daughter ion, which corroborates the loss of ^{18}O-incorporated CO_2 during CID-induced decarboxylation. This analysis confirms that, after first oxidation of Ser to FGly, SjiB-399 can further oxidize the hydrated FGly (i.e. *gem*-diol) to produce Ama (Figure 3B). Incorporation of two ^{18}O atoms into Ama is apparently owing to solvent exchange via the equilibrium of aldehyde and *gem*-diol,[46] and the latter is oxidized to Ama.

Re-examination of in vivo data revealed Ama was also produced in the co-expression study, which is ≈30-fold lower than that of the cyclophane product (Figure S11 and S17). We also carried out a set of in vivo and in vitro experiments in different conditions. This analysis showed that although increasing co-expression time did not significantly change the ratio of the products, apparently increased yield of the Ama product was observed with prolonged reaction time in vitro; in this condition, the cross-linked cyclophane product was still not observed (Figure S17). The factors that contribute to the distinct reaction outcomes between in vivo and in vitro assays remain unknown and is under investigation in our laboratory. Despite this, the data presented herein clearly demonstrated that Ama can be produced by posttranslational oxidation of Ser, shedding lights on the elusive origin of Ama in Nature.

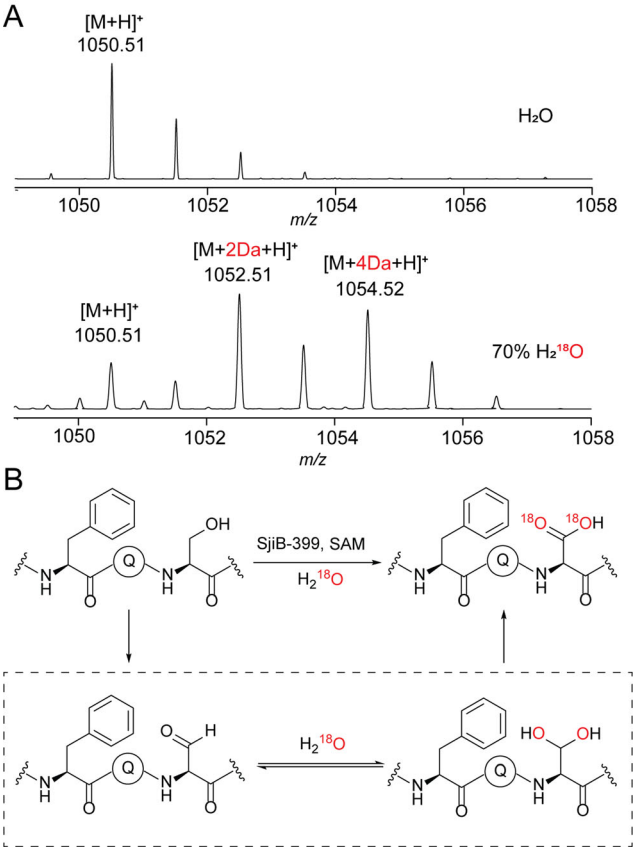

Figure 3. Enzymatic Ama formation in SjiA. A. HR-MS analysis of the Ama product derived from in vitro enzymatic assays in H_2O or 70% $H_2{}^{18}O$, showing up to two ^{18}O atoms were incorporated into the Ama product. B. Reaction Scheme of the SjiB-399-catalyzed Ama formation, highlighting the oxidation proceeds in a solvent-exchangeable manner (dashed box).

3-CyFEs are Phylogenetically Closely Related to anSMEs

The fact that SjiB-399 also serves as a robust serine oxidase intrigued us to carry out extensive bioinformatic analysis. Using SjiB-399 as a sequence query, we performed five rounds of position specific iterated (PSI)-BLAST in RefSeq database. The resulting homologs ($n = 5000$) were analyzed by RODEO[47] to retrieve Pfam and TIGRFAM annotation of surrounding genes. Surprisingly, in addition to ≈3800 3-CyFEs that are encoded within the apparent triceptide BGCs, we noticed ≈1000 proteins belonging to the anSME protein family (TIGR03942). Most of these putative anSMEs ($n = 801$) are encoded next to a ≈600 aa protein annotated as "sulfatase" (PF00884) or "chol sulfatase: choline-sulfatase" (TIGR03417) (Supporting Information). These sulfatase-like sequences possess the characteristic substrate motif (C/S)*x*(P/A)xR as described previously (Supporting Information),[42] suggesting that they are bona fide anaerobic sulfatases that could be post-translationally modified by the corresponding anSMEs. This survey indicates 3-CyFEs bear significant sequence homology to anSMEs involved in anaerobic sulfatase maturation. We noted that the rSAM enzymes involved in the biosynthesis of other RiPP classes were not found in this BLASTp search.

To further gain insights into the phylogenetic relationship between 3-CyFE and anSMEs, we constructed a rooted maximum likelihood (ML) phylogenetic tree using selected sequences from the dataset (Supporting Information). The known rSAMs involved in the biosynthesis of ranthipeptide, sactipeptide and shp/rgg-associated cyclic peptides were manually incorporated into this analysis. The result showed that anSMEs and 3-CyFEs fall into the same major clade in the phylogenetic tree (Figure 4 A). Sequence similarity network (SSN) analysis verifies that 3-CyFEs are more related to anSMEs, in stark contrast to other known RiPP-modifying rSAMs that form C–O, C–C, C–-S crosslinks (Figure S18). These analyses indicated that anSMEs and 3-CyFEs likely have evolved from the same ancestor; both groups of enzymes are phylogenetically distantly related to other known RiPP-modifying rSAM enzymes.

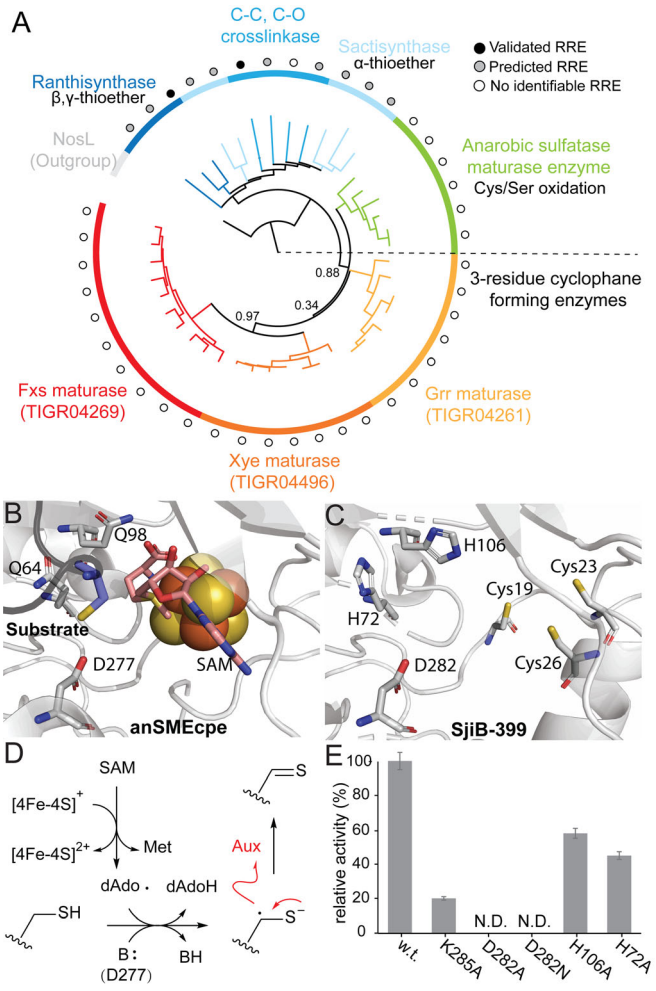

Figure 4. 3-CyFEs are close homologs of anSMEs. A. Maximum likelihood (ML) phylogenetic tree of 3-CyFEs, anSMEs and other known RiPP-modifying rSAM enzymes. The tree is rooted using tryptophan lyase NosL.[51] Key bootstrap values are indicated along the branch. B. The active site of anSMEcpe (PDB: 4K39), showing the rSAM cluster, SAM, catalytic residues and the substrate peptide with Cys highlighted in sticks. C. The homology structure of SjiB-399 using anSMEcpe as the structure template. Shown is the same view as that in B. D. The proposed catalytic mechanism of anSMEcpe, in which the conserved D277 serves as a base to deprotonate substrate Cys. Aux, auxiliary [4Fe-4S] clusters. E. Site-directed mutagenesis and the resulting activity for SjiB-399. The activity is assessed by LC-HRMS and quantified by the relative EIC area of all products versus the unmodified precursor peptide. See Figure S21C for the detailed ratio of each product.

Extensive efforts to crystalize SjiB-399 prove to be unsuccessful. However, we noted that, anSMEcpe,[42] an anSME that modifies a Cys-type sulfatase, displays apparent sequence homology to SjiB-399 (26% identity and 41% similarity, Figure S19), and its crystal structure is available (PDB: 4K39). We hence constructed a homology model of SjiB-399, which consists of an N-terminal rSAM domain and a C-terminal SPASM domain (Figure S20). C323, C329, C335 and C365 in the SPASM domain are highly conserved among 3-CyFEs. These four Cys residues are likely involved in coordinating an auxiliary [4Fe-4S] cluster (referred to as 3-CyFE Aux cluster), which is equivalent to the AuxII cluster of anSMEcpe. We noted that SjiB-399 and other 3-CyFEs lack the other four Cys residues in anSMEcpe for ligating the AuxI cluster, and this finding is consistent with the in vitro Fe/S quantification analysis showing that SjiB-399 only has two [4Fe-4S] clusters (i.e. a rSAM cluster and an auxiliary cluster). We respectively changed C19, C329 and C364 to Ala and co-expressed each of these mutants with SjiA. The results showed that the enzyme activity was completely abolished in all the three mutants (Figure S16), indicating both [4Fe-4S] clusters are strictly essential for enzyme activity.

Careful inspection of the putative catalytic site of SjiB-399 reveals that H72, H106 and D282 (Figure 5 C and Figure S21) appear to be equivalent to the Q64, Q98 and D277 found in anSMEcpe (Figure 5 B). In anSMEcpe, D277 likely serves as a general base to deprotonate Cys thiol (Figure 5 D), while Q64 and Q98 are suggested to stabilize the catalytic D277, and participate in substrate binding and orientation.[42] We constructed the H72A, H106A, D282A and D282N mutants and co-expressed each mutant with SjiA. The result (Figure 5 E) clearly shows that both D282A and D282N are completely inactive, demonstrating the strictly essential role of Asp282 in catalysis (Figure S22). In contrast, H72A and H106A are still able to produce both cyclophane and FGly product, albeit with diminished activity, suggesting these two His residue is not strictly essential. Further inspection into the multiple sequence alignment of Fxs-type 3-CyFEs also reveals a highly conserved Lys residue K285 (Figure S19 and Figure S21), but changing this residue to Ala only partially decreased enzyme activity. Ama production was not observed in all these analyses.

Substrate-Tuned Partition of Divergent Pathways in SjiB-399 Catalysis

Given the remarkable catalytic promiscuity of SjiB-399, we envisioned that proper variation of the substrate motif Ω1-X2-S3 may alter the reaction paths (Figure 5 A). To test this hypothesis, we first conducted a thorough mining of the putative substrates of the FxsB-type 3-CyFEs. By aligning to the profile hidden Markov model (HMM) of FxsA (TIGR04268), we generated a comprehensive list of substrate candidates containing ≈1000 sequences (Supporting Information), which can be classified into 23 major groups based on SSN analysis (Figure S23-S24). Careful inspection of these

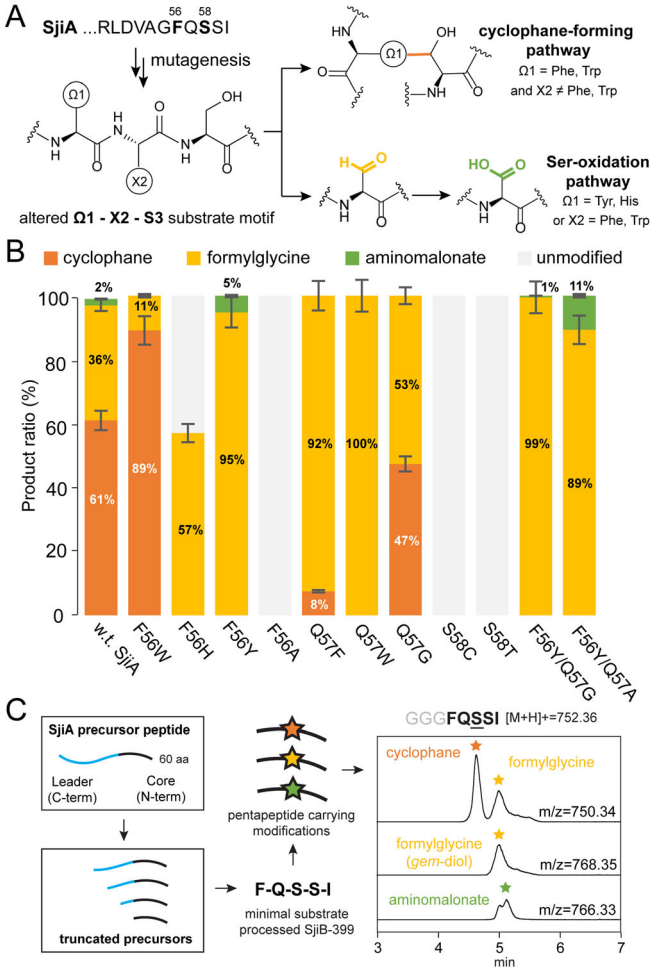

Figure 5. Substrate-tuned and leader-independent peptide modification by SjiB-399. A. A general reaction Scheme showing that the modification outcome of SjiB-399 is highly dependent on the substrate motif Ω1-X2-S3. B. Product ratio of various SjiA precursor mutants co-expressed with SjiB-399. Data are mean ± s.d. of biological replicates ($n=3$). For product titer (μg per liter culture), see Table S3. Note the formylglycine product was calculated incorporating its hydrated form (i.e. the *gem-diol* counterpart). C. The leader peptide-independent reaction of SjiB-399, showing the co-expression analysis with various truncated SjiA peptides. The minimal substrate that can be processed SjiB-399 is FQSSI and the EIC traces for the three products are indicated (the Ser subjected to modification is underlined). Note the GGG in gray is a linker released from maltose binding protein (MBP) tag by TEV protease digestion (Supporting Information).

sequence patterns revealed that the conserved Phe in the FxS motif can be substituted with Trp, Tyr and His, while the substrate Ser can be substituted with Asn and Thr (Figure S25). The X2 residue is more divergent, including Asn, Asp, Gln, and Glu, although other residues such as Ala, Val are also found.

We next changed the Phe in SjiA to its natural substitutes (i.e. Trp, Tyr and His), and the mutants were each co-expressed with SjiB-399 in *E. coli.* Interestingly, although for F56W, the cyclophane product remained predominant (Figure S27-S28), the F56Y and F56H mutants were all switched to the Ser oxidation pathways (Figure 5B, Figure S26-S32). In F56H, only ≈50% of substrate was converted to FGly and *gem*-diol (Figure S29-S30), whereas no Ama product is observed, indicating His at the Ω1 position is less favorable in the *sji* system. In contrast, the F56Y mutant was fully modified, affording ≈5% Ama product and ≈95% FGly and *gem*-diol products (Figure S26-S28). The F56Y mutant was also co-expressed with SjiB-399 D282N; however, no modification occurs, which further supports the indispensable role of D282 in SjiB-399 catalysis (Figure S22).

We further changed Phe56 to Ala and conducted co-expression analysis. No modification of the F56A mutant was observed (Figure S44), indicating the aromatic Ω1 residue is indispensable for enzyme processing. We also constructed the S58C and S58T mutants, but no modification was observed for these two mutants (Figure S44), indicating the *sji* system can only specifically modify a Ser residue within the Ω1-X2-S3 motif.

Because aromatic residues are not found in the X2 position (Figure S25), we constructed a Q57F mutant to interrogate whether the enzyme can accept aromatic residues at this position. Moreover, the resulting mutant has a FFSS motif in the C-terminus, which is actually an overlap of two FxS motifs. Subsequent analysis showed that the Q57F mutant was mostly converted to the FGly product, and the cyclophane product is insignificant (Figure 5B, Figure S33-S34). Notably, although two overlapped FxS motifs are present in FFSS, HR-MS/MS analysis showed that modification occurs exclusively on the first Ser residue (i.e. the native substrate Ser58) (Figure S34), indicating the enzymatic process is strictly site-specific. Similarly, the Q57W mutant peptide is completely modified to the FGly product whereas the cyclophane product is not observed (Figure 5B, Figure S35-S36). These results indicated that the big steric aromatic residue at the X2 position can block the cyclophane-forming pathway between Ω1 and S3, thereby only allow for Ser oxidation. We also changed Gln57 to Gly, and the Q57G mutant was found to be roughly equally partitioned into both cyclophane and FGly pathways (Figure 5B, Figure S37-S38).

We also investigated the modification in the double mutants. These analyses showed that cyclophane formation was fully abolished in the F56Y/Q57G mutant, which was completely converted to the FGly/*gem*-diol product (Figure 5B, Figure S39-S40). Intriguingly, we observed significantly enhanced production of Ama in the F56Y/Q57A mutant, which accounts for more than 10% of conversion (Figure 5B, Figure S41-43). On the contrary, Ama production is barely observed for the F56Y/Q57G mutant.

SjiA Modification by SjiB-399 is Leader Peptide-Independent

Because anSMEs are active on short oligopeptides derived from the native substrate,[40] the close phylogeny between 3-CyFEs and anSMEs suggests that 3-CyFEs may also do not require leader peptide for activity. To test this hypothesis, we constructed a series of SjiA truncation mutants by removing the 15, 25, 30, 40, 45, 49 and 55 amino acids at the N-terminus, respectively, which were then co-expressed with SjiB-399. Remarkably, we found that all the truncated

mutants were fully modified by the enzyme, even for the pentapeptide FQSSI, which lacks the N-terminal 55 aa (Figure 5C, Figure S45). These results are consistent with observation that the 23 groups of precursor peptides mined in this study lack the overall similarity in the N-terminal region (Figure S19-S20). Importantly, these results are consistent with the fact that no RRE was found in relation to 3-CyFEs, which are potentially interesting for future endeavors in protein engineering and peptide modification.

Conclusion

In this study, we showed that a FxS-type 3-CyFE exhibits remarkable catalytic promiscuity, which not only produces the cyclized cyclophane product but also carries out Ser oxidation to produce FGly and Ama. Catalytic promiscuity has recently been reported for several rSAM proteins, and in most cases, the promiscuous activities are associated with unnatural substrates.[48–56] The tryptophan lyase NosL[57–59] and the anaerobic coproporphyrinogen III oxidase HemN[60] are exceptional examples in which promiscuous activity were observed with native substrates. By characterization of the Ser oxidation activity of SjiB-399, our study adds a new example to these exceptions. These findings highlight the remarkable catalytic plasticity of the rSAM enzymes and the great potential to engineer these catalysts for novel activities.

Our study also represents the first report of Ama production in a ribosomal peptide. It has long been proposed that Ama could be produced by post-translational modification,[13] but this hypothesis remains only speculative. Our study validates the possibility of the post-translationally produced Ama and sheds lights on the biosynthetic origin of this widespread structural moiety in biological systems. Our work also demonstrates the rich chemistry in RiPP biosynthesis and the fascinating opportunity to expand chemical diversity by engineering RiPP biosynthetic pathways.

Acknowledgements

This work is supported in part by grants from the National Key Research and Development Program (2016 Y F A0501302 and 2018Y F A0900402), from National Natural Science Foundation of China (21822703, 21921003, and 32070050), and from Innovative research team of high-level local universities in Shanghai.

Conflict of Interest

The authors declare no conflict of interest.

Keywords: anaerobic sulfatase maturase · gem-diol · oxidation · posttranslational modification · RiPP

[1] K. Shimura, H. Nagayama, A. Kikuchi, *Nature* **1956**, *177*, 935–936.
[2] H. Nagayama, M. Muramatsu, K. Shimura, *Nature* **1958**, *181*, 417–418.
[3] I. Ciciliato, E. Corti, E. Sarubbi, S. Stefanelli, L. Gastaldo, N. Montanini, M. Kurz, D. Losi, F. Marinelli, E. Selva, *J. Antibiot.* **2004**, *57*, 210–217.
[4] A. W. Sangster, S. E. Thomas, N. L. Tingling, *Tetrahedron* **1975**, *31*, 1135–1137.
[5] H. B. Park, J. M. Crawford, *J. Nat. Prod.* **2015**, *78*, 1437–1441.
[6] J. G. Batelaan, J. W. F. K. Barnick, J. L. van der Baan, F. Bickelhaupt, *Tetrahedron Lett.* **1972**, *13*, 3107–3110.
[7] B. J. C. Law, Y. Zhuo, M. Winn, D. Francis, Y. X. Zhang, M. Samborskyy, A. Murphy, L. J. Ren, P. F. Leadlay, J. Micklefield, *Nat. Catal.* **2018**, *1*, 977–984.
[8] A. O. Brachmann, C. Garcie, V. Wu, P. Martin, R. Ueoka, E. Oswald, J. Piel, *Chem. Commun.* **2015**, *51*, 13138–13141.
[9] Y. A. Chan, M. G. Thomas, *Biochemistry* **2010**, *49*, 3667–3677.
[10] Y. A. Chan, M. T. Boyne 2nd, A. M. Podevels, A. K. Klimowicz, J. Handelsman, N. L. Kelleher, M. G. Thomas, *Proc. Natl. Acad. Sci. USA* **2006**, *103*, 14349–14354.
[11] Y. A. Chan, A. M. Podevels, B. M. Kevany, M. G. Thomas, *Nat. Prod. Rep.* **2009**, *26*, 90–114.
[12] J. J. Van Buskirk, W. M. Kirsch, D. L. Kleyer, R. M. Barkley, T. H. Koch, *Proc. Natl. Acad. Sci. USA* **1984**, *81*, 722–725.
[13] S. D. Copley, E. Frank, W. M. Kirsch, T. H. Koch, *Anal. Biochem.* **1992**, *201*, 152–157.
[14] P. G. Arnison, M. J. Bibb, G. Bierbaum, A. A. Bowers, T. S. Bugni, G. Bulaj, J. A. Camarero, D. J. Campopiano, G. L. Challis, J. Clardy, P. D. Cotter, D. J. Craik, M. Dawson, E. Dittmann, S. Donadio, P. C. Dorrestein, K. D. Entian, M. A. Fischbach, J. S. Garavelli, U. Goransson, C. W. Gruber, D. H. Haft, T. K. Hemscheidt, C. Hertweck, C. Hill, A. R. Horswill, M. Jaspars, W. L. Kelly, J. P. Klinman, O. P. Kuipers, A. J. Link, W. Liu, M. A. Marahiel, D. A. Mitchell, G. N. Moll, B. S. Moore, R. Muller, S. K. Nair, I. F. Nes, G. E. Norris, B. M. Olivera, H. Onaka, M. L. Patchett, J. Piel, M. J. Reaney, S. Rebuffat, R. P. Ross, H. G. Sahl, E. W. Schmidt, M. E. Selsted, K. Severinov, B. Shen, K. Sivonen, L. Smith, T. Stein, R. D. Sussmuth, J. R. Tagg, G. L. Tang, A. W. Truman, J. C. Vederas, C. T. Walsh, J. D. Walton, S. C. Wenzel, J. M. Willey, W. A. van der Donk, *Nat. Prod. Rep.* **2013**, *30*, 108–160.
[15] M. Montalbán-López, T. A. Scott, S. Ramesh, I. R. Rahman, A. J. van Heel, J. H. Viel, V. Bandarian, E. Dittmann, O. Genilloud, Y. Goto, M. J. Grande Burgos, C. Hill, S. Kim, J. Koehnke, J. A. Latham, A. J. Link, B. Martínez, S. K. Nair, Y. Nicolet, S. Rebuffat, H. G. Sahl, D. Sareen, E. W. Schmidt, L. Schmitt, K. Severinov, R. D. Süssmuth, A. W. Truman, H. Wang, J. K. Weng, G. P. van Wezel, Q. Zhang, J. Zhong, J. Piel, D. A. Mitchell, O. P. Kuipers, W. A. van der Donk, *Nat. Prod. Rep.* **2020**, *38*, 130–239.
[16] K. Yokoyama, E. A. Lilla, *Nat. Prod. Rep.* **2018**, *35*, 660–694.
[17] N. Mahanta, G. A. Hudson, D. A. Mitchell, *Biochemistry* **2017**, *56*, 5229–5244.
[18] T. Mo, X. Ji, W. Yuan, D. Mandalapu, F. Wang, Y. Zhong, F. Li, Q. Chen, W. Ding, Z. Deng, S. Yu, Q. Zhang, *Angew. Chem. Int. Ed.* **2019**, *58*, 18793–18797; *Angew. Chem.* **2019**, *131*, 18969–18973.
[19] L. B. Bushin, B. C. Covington, B. E. Rued, M. J. Federle, M. R. Seyedsayamdost, *J. Am. Chem. Soc.* **2020**, *142*, 16265–16275.
[20] S. Chiumento, C. Roblin, S. Kieffer-Jaquinod, S. Tachon, C. Lepretre, C. Basset, D. Aditiyarini, H. Olleik, C. Nicoletti, O. Bornet, O. Iranzo, M. Maresca, R. Hardre, M. Fons, T. Giardina, E. Devillard, F. Guerlesquin, Y. Coute, M. Atta, J. Perrier, M. Lafond, V. Duarte, *Sci. Adv.* **2019**, *5*, eaaw9969.
[21] G. A. Hudson, B. J. Burkhart, A. J. DiCaprio, C. J. Schwalen, B. Kille, T. V. Pogorelov, D. A. Mitchell, *J. Am. Chem. Soc.* **2019**, *141*, 8228–8238.

[22] Y. Chen, Y. Yang, X. Ji, R. Zhao, G. Li, Y. Gu, A. Shi, W. Jiang, Q. Zhang, *Biotechnol. J.* **2020**, e2000136.
[23] A. Caruso, L. B. Bushin, K. A. Clark, R. J. Martinie, M. R. Seyedsayamdost, *J. Am. Chem. Soc.* **2019**, *141*, 990 – 997.
[24] K. R. Schramma, L. B. Bushin, M. R. Seyedsayamdost, *Nat. Chem.* **2015**, *7*, 431 – 437.
[25] K. A. Clark, L. B. Bushin, M. R. Seyedsayamdost, *J. Am. Chem. Soc.* **2019**, *141*, 10610 – 10615.
[26] A. Caruso, R. J. Martinie, L. B. Bushin, M. R. Seyedsayamdost, *J. Am. Chem. Soc.* **2019**, *141*, 16610 – 16614.
[27] H. J. Sofia, G. Chen, B. G. Hetzler, J. F. Reyes-Spindola, N. E. Miller, *Nucleic Acids Res.* **2001**, *29*, 1097 – 1106.
[28] W. E. Broderick, B. M. Hoffman, J. B. Broderick, *Acc. Chem. Res.* **2018**, *51*, 2611 – 2619.
[29] T. A. Grell, P. J. Goldman, C. L. Drennan, *J. Biol. Chem.* **2015**, *290*, 3964 – 3971.
[30] D. H. Haft, M. K. Basu, *J. Bacteriol.* **2011**, *193*, 2745 – 2755.
[31] T. Q. N. Nguyen, Y. W. Tooh, R. Sugiyama, T. P. D. Nguyen, M. Purushothaman, L. C. Leow, K. Hanif, R. H. S. Yong, I. Agatha, F. R. Winnerdy, M. Gugger, A. T. Phan, B. I. Morinaka, *Nat. Chem.* **2020**, *12*, 1042—1053.
[32] B. J. Burkhart, G. A. Hudson, K. L. Dunbar, D. A. Mitchell, *Nat. Chem. Biol.* **2015**, *11*, 564 – 570.
[33] A. M. Kloosterman, K. E. Shelton, G. P. van Wezel, M. H. Medema, D. A. Mitchell, *mSystems* **2020**, *5*, e00267-20.
[34] T. W. Precord, N. Mahanta, D. A. Mitchell, *ACS Chem. Biol.* **2019**, *14*, 1981 – 1989.
[35] E. L. Morinaka, M. Verest, M. J. Helf, T. Scalvenzi, A. L. Vagstad, J. Sims, S. Sunagawa, M. Gugger, J. Piel, *Science* **2018**, *359*, 779 – 782.
[36] L. B. Bushin, K. A. Clark, I. Pelczer, M. R. Seyedsayamdost, *J. Am. Chem. Soc.* **2018**, *140*, 17674 – 17684.
[37] J. A. Latham, A. T. Iavarone, I. Barr, P. V. Juthani, J. P. Klinman, *J. Biol. Chem.* **2015**, *290*, 12908 – 12918.
[38] N. M. Hooper, *FEBS Lett.* **1994**, *354*, 1 – 6.
[39] Y. Huang, Q. Cui, L. Wang, C. Rodriguez, E. Quintana, M. Goodfellow, Z. Liu, *Antonie Van Leeuwenhoek* **2004**, *86*, 159 – 165.
[40] T. L. Grove, K. H. Lee, J. St Clair, C. Krebs, S. J. Booker, *Biochemistry* **2008**, *47*, 7523 – 7538.
[41] A. Benjdia, S. Subramanian, J. Leprince, H. Vaudry, M. K. Johnson, O. Berteau, *FEBS J.* **2010**, *277*, 1906 – 1920.
[42] P. J. Goldman, T. L. Grove, L. A. Sites, M. I. McLaughlin, S. J. Booker, C. L. Drennan, *Proc. Natl. Acad. Sci. USA* **2013**, *110*, 8519 – 8524.
[43] T. B. Moyer, N. C. Parsley, P. W. Sadecki, W. J. Schug, L. M. Hicks, *Nat. Prod. Rep.* **2021**, *38*, 489 – 509.
[44] J. W. Thanassi, *Biochemistry* **1970**, *9*, 525 – 532.
[45] P. Wheelan, W. M. Kirsch, T. H. Koch, *J. Org. Chem.* **1989**, *54*, 1364 – 1370.
[46] J. Wang, S. Ma, W. Ding, T. Chen, Q. Zhang, *Chin. J. Chem.* **2021**, *39*, 1923 – 1926.
[47] J. I. Tietz, C. J. Schwalen, P. S. Patel, T. Maxson, P. M. Blair, H. C. Tai, U. I. Zakai, D. A. Mitchell, *Nat. Chem. Biol.* **2017**, *13*, 470 – 478.
[48] W. Ding, X. Ji, Y. Zhong, K. Xu, Q. Zhang, *Curr. Opin. Chem. Biol.* **2020**, *55*, 86 – 95.
[49] N. A. Bruender, T. A. Grell, D. P. Dowling, R. M. McCarty, C. L. Drennan, V. Bandarian, *J. Am. Chem. Soc.* **2017**, *139*, 1912 – 1920.
[50] A. Silakov, T. L. Grove, M. I. Radle, M. R. Bauerle, M. T. Green, A. C. Rosenzweig, A. K. Boal, S. J. Booker, *J. Am. Chem. Soc.* **2014**, *136*, 8221 – 8228.
[51] M. Dong, M. Horitani, B. Dzikovski, M. E. Pandelia, C. Krebs, J. H. Freed, B. M. Hoffman, H. Lin, *J. Am. Chem. Soc.* **2016**, *138*, 9755 – 9758.
[52] M. Dong, M. Horitani, B. Dzikovski, J. H. Freed, S. E. Ealick, B. M. Hoffman, H. Lin, *J. Am. Chem. Soc.* **2017**, *139*, 5680 – 5683.
[53] S. Joshi, N. Mahanta, D. Fedoseyenko, H. Williams, T. P. Begley, *J. Am. Chem. Soc.* **2017**, *139*, 10952 – 10955.
[54] X. Ji, D. Mandalapu, J. Cheng, W. Ding, Q. Zhang, *Angew. Chem. Int. Ed.* **2018**, *57*, 6601 – 6604; *Angew. Chem.* **2018**, *130*, 6711 – 6714.
[55] S. Ghosh, E. N. G. Marsh, *J. Biol. Chem.* **2020**, *295*, 11513 – 11528.
[56] D. Y. Yin, X. Ji, Q. Zhang, *Chin. J. Chem.* **2021**, https://doi.org/10.1002/cjoc.202100304.
[57] D. M. Bhandari, D. Fedoseyenko, T. P. Begley, *Methods Enzymol.* **2018**, *606*, 155 – 178.
[58] W. Ding, X. Ji, Y. Li, Q. Zhang, *Front. Chem.* **2016**, *4*, 27.
[59] G. Sicoli, J. M. Mouesca, L. Zeppieri, P. Amara, L. Martin, A. L. Barra, J. C. Fontecilla-Camps, S. Gambarelli, Y. Nicolet, *Science* **2016**, *351*, 1320 – 1323.
[60] X. Ji, T. Mo, W. Q. Liu, W. Ding, Z. Deng, Q. Zhang, *Angew. Chem. Int. Ed.* **2019**, *58*, 6235 – 6238; *Angew. Chem.* **2019**, *131*, 6301 – 6304.

Manuscript received: May 29, 2021
Revised manuscript received: June 23, 2021
Accepted manuscript online: June 24, 2021
Version of record online: ■■ ■■, ■■■■

Research Articles

Biosynthesis

S. Ma, H. Chen, H. Li, X. Ji, Z. Deng, W. Ding, Q. Zhang* ——— ■■■■–■■■■

Post-Translational Formation of Aminomalonate by a Promiscuous Peptide-Modifying Radical SAM Enzyme

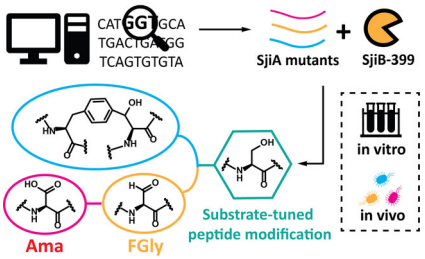

We report biochemical study of a radical S-adenosylmethionine (rSAM) enzyme involved in the biosynthesis of a ribosomally synthesized and post-translationally modified peptide (RiPP). This rSAM enzyme exhibits remarkable catalytic promiscuity, which produces cyclophane in vivo but formylglycine and aminomalonate (Ama) in vitro. Unlike most enzymes involved in RiPP biosynthesis, this enzyme does not require leader peptide for activity.